ACIS QE: Investigating the BI/FI Ratio

- Grating & Cluster data want BI/FI ratio higher than CALDB
- Size of effect: $\sim 10 - 15\%$
- wavelength dependent, especially notable for $E < 1.5$ keV.
- Absolute calibration from ground (XRCF) data may settle the issue

Two effects:

- Dead area due to cosmic ray blooms: larger effect on FI than BI (See Yousaf Butt's talk, this meeting)
- Reassessment of QE at low energies.

This investigation is in response to two action items from the 2002 Nov Calibration Workshop.

- Also: Quantum Efficiency Uniformity, a reassessment.

Re-analysis of XRCF Flat Field data at low energies

- Better modelling of spectral features, teasing apart continua and lines.
- Accounts for non-Gaussian line shapes, especially important at low energies.
- Comparison to synchrotron-calibrated Flow Proportional Counter in same beam

	Oxygen	Copper
energy	**0.5249 keV**	**0.9297 keV**
	measured	
QE(S2)	0.228 ± 0.005	0.558 ± 0.014
QE(S3)	0.615 ± 0.013	0.841 ± 0.024
S3/S2	2.697 ± 0.0772	1.508 ± 0.0577
	CALDB	
QE(S2)	**0.2120**	**0.5644**
QE(S2)	**0.5230**	**0.7861**
S3/S2	**2.467**	**1.3928**
XRCF/CALDB	$1.093 \pm .0313$	1.083 ± 0.041
CALDB/XRCF	0.915 ± 0.026	0.9234 ± 0.035
ground corrected r/y	0.900 ± 0.05	0.946 ± 0.05

- Agreement between last 2 rows is good.

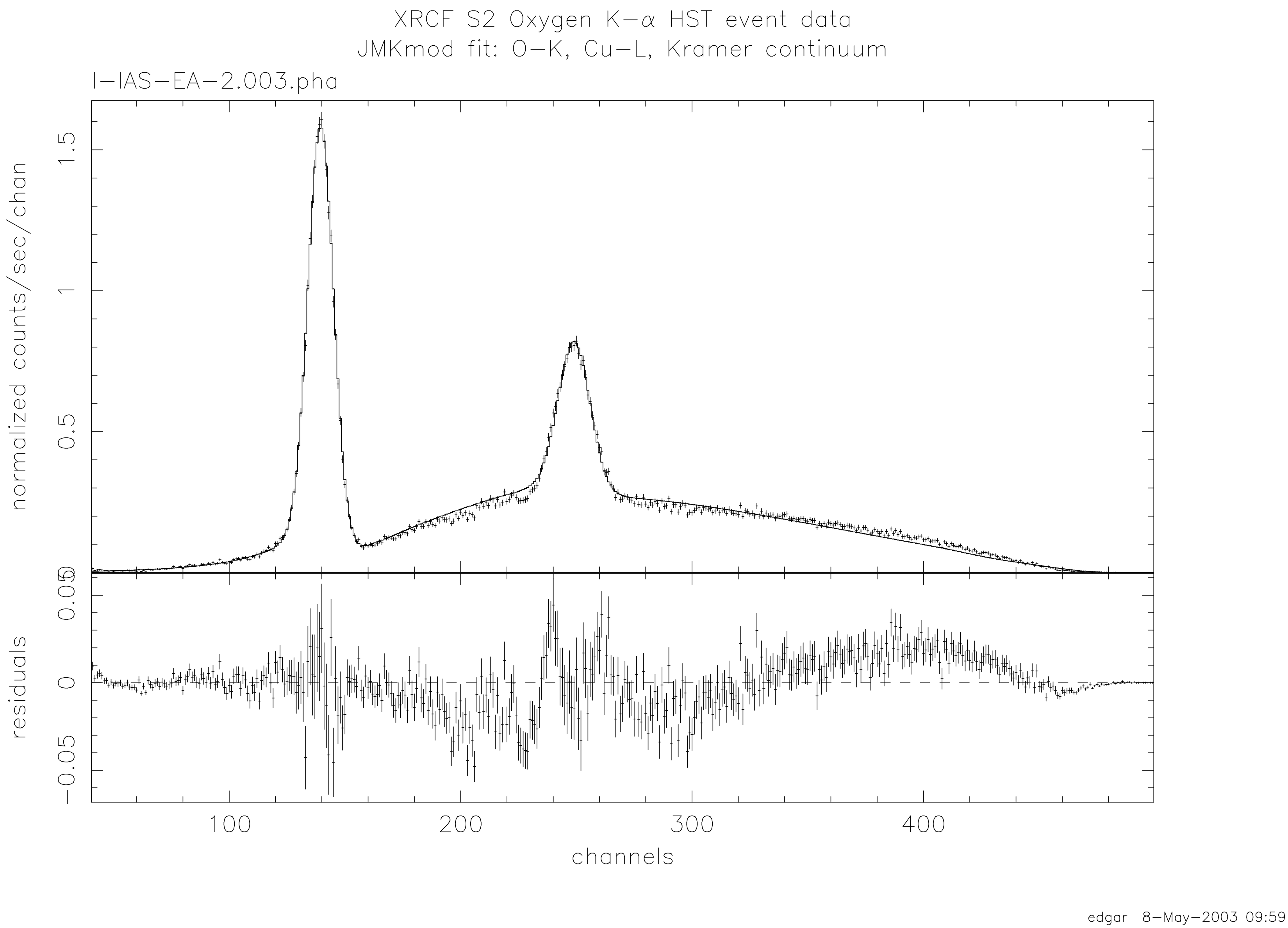

Figure 1: Fitted pulse-height spectrum for S2 (full chip).

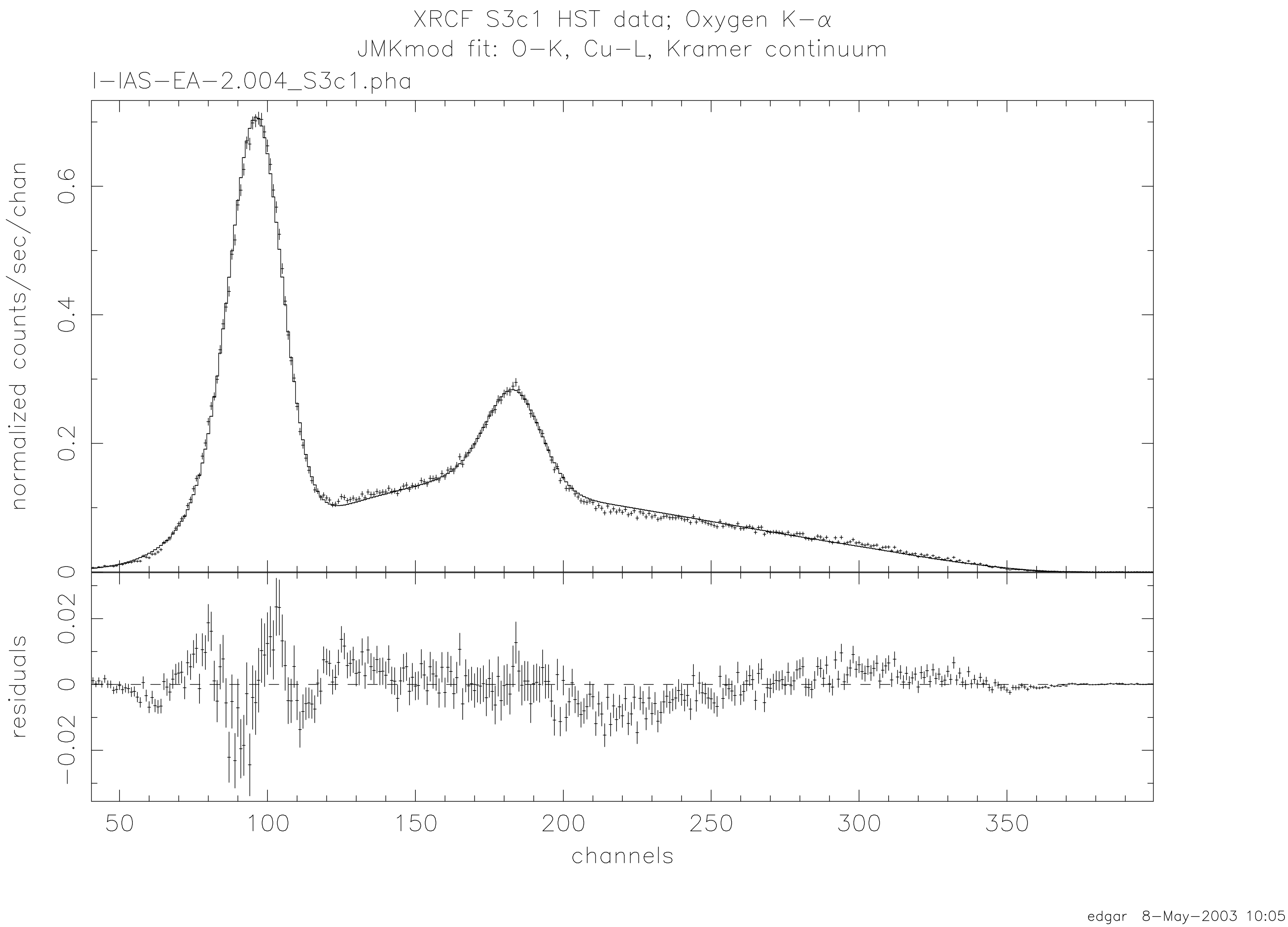

Figure 2: Fitted pulse-height spectrum for S3 (node 1).

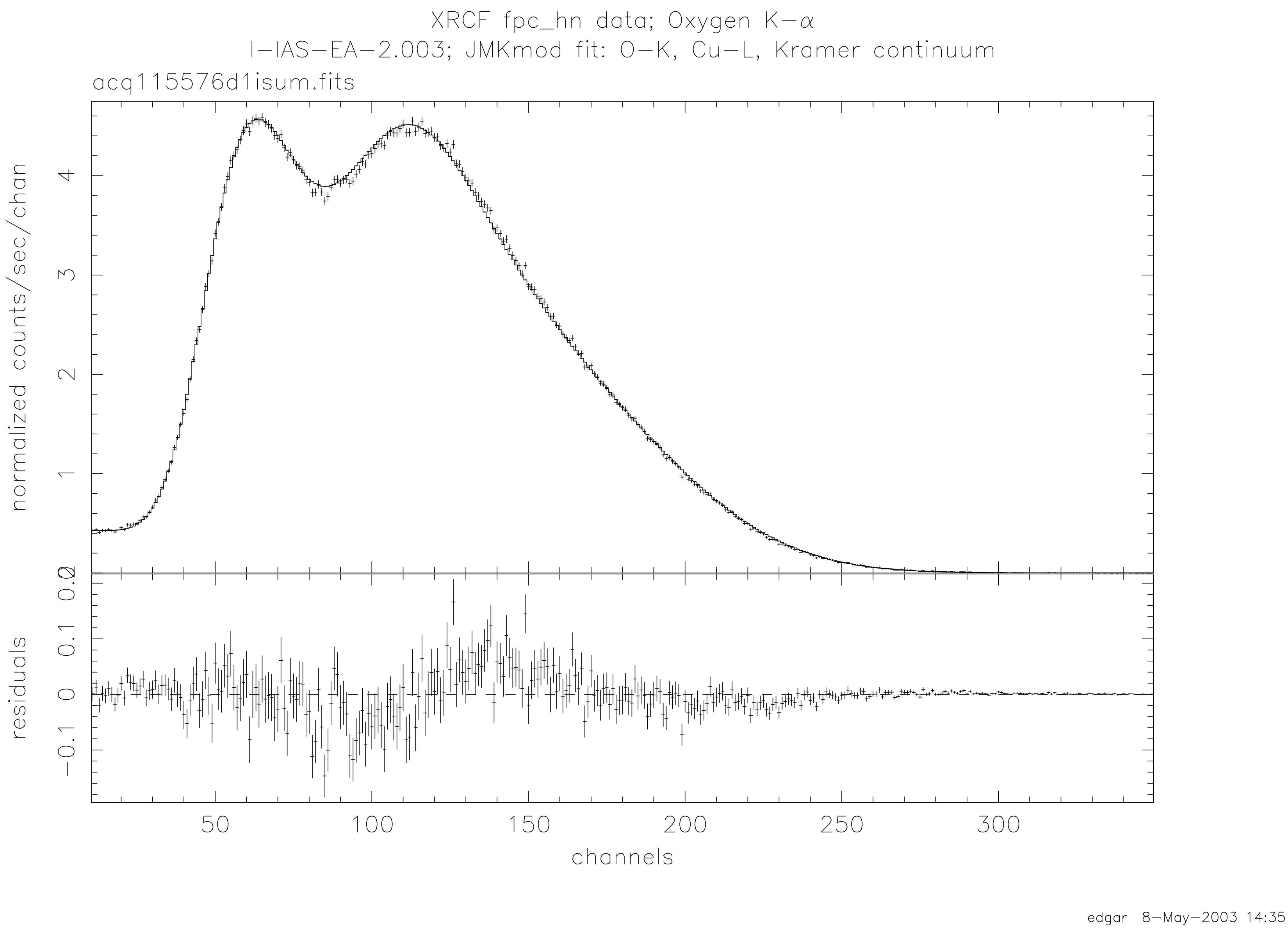

Figure 3: Fitted pulse-height spectrum for FPC_HN.

ACIS QE: BI/FI from XRCF data
30 October 2001

For each detector, the source luminosity is given by:

$$S = \frac{C_{det}}{A_{det} QE_{det}} \times d_{det}^2 BU_{det}$$

where:

- C = **countrate in the line** (cts s^{-1})
- A = **active detector area** (cm^2)
- QE = **quantum efficiency** (cts $photon^{-1}$)
- d = **source distance** (cm)
- BU = **Beam Uniformity factor (dimensionless).**

Then:

$$QE_{ACIS} = QE_{hn} \times \frac{C_{ACIS}}{C_{hn}} \times \frac{A_{hn}}{A_{ACIS}} \times \frac{BU_{ACIS}}{BU_{hn}} \times \frac{d_{ACIS}^2}{d_{hn}^2}$$

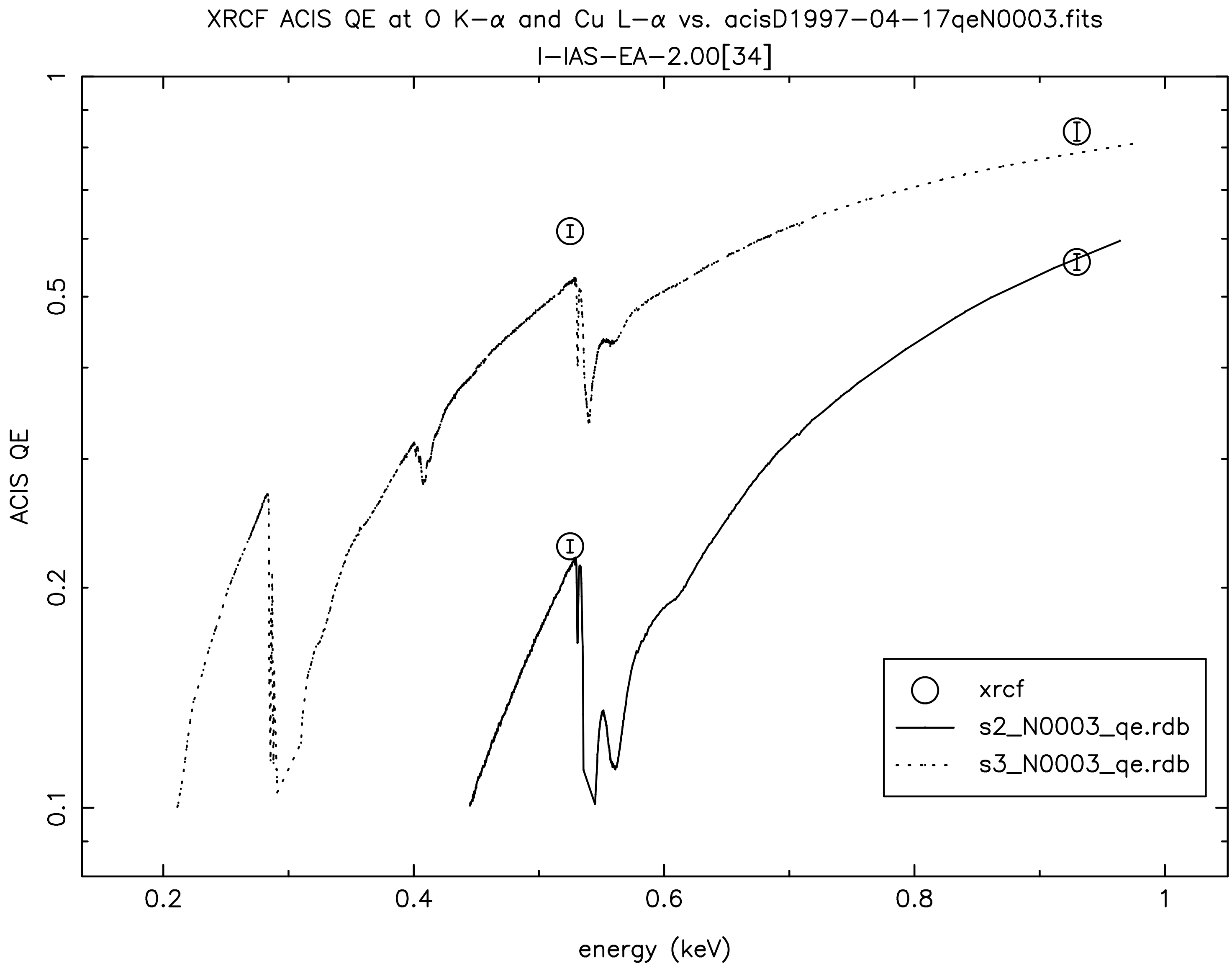

Figure 4: S2 and S3 quantum efficiency from CALDB N0003 (curves) and measured (data points).

Results in Context
28 October 2003

- Marshall defines

$$r(\lambda) \equiv \frac{(QE_{FI}/QE_{BI})_{true}}{(QE_{FI}/QE_{BI})_{caldb}}$$

- This is his proposed correction to the FI QE curve (see fig 5).
- Since based on flight data, r includes a factor of the FI cosmic ray QE decrement $y = 0.9632$.
- FOR COMPARISON TO GROUND DATA ONLY, we will correct QE(S3) by factor y/r. (See fig 6)

Recommendations for flight calibration products:

- Decrement FI QE curves by factor y at all energies.
- Increase BI QE curves by factor consistent with y/r (but details of energy dependence TBD).

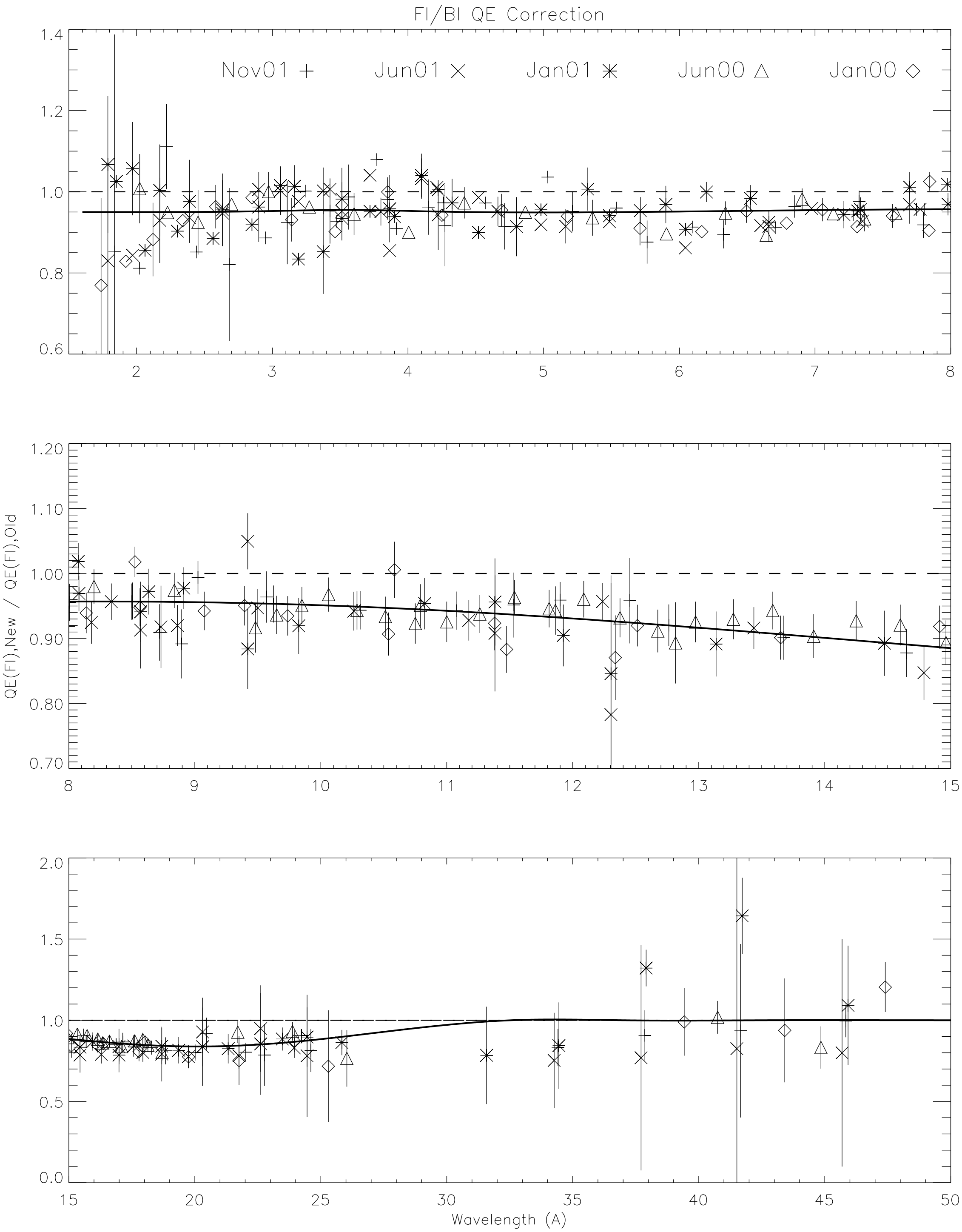

Figure 5: Marshall's plot of r vs. wavelength. This is his proposed correction to the FI QE curve.

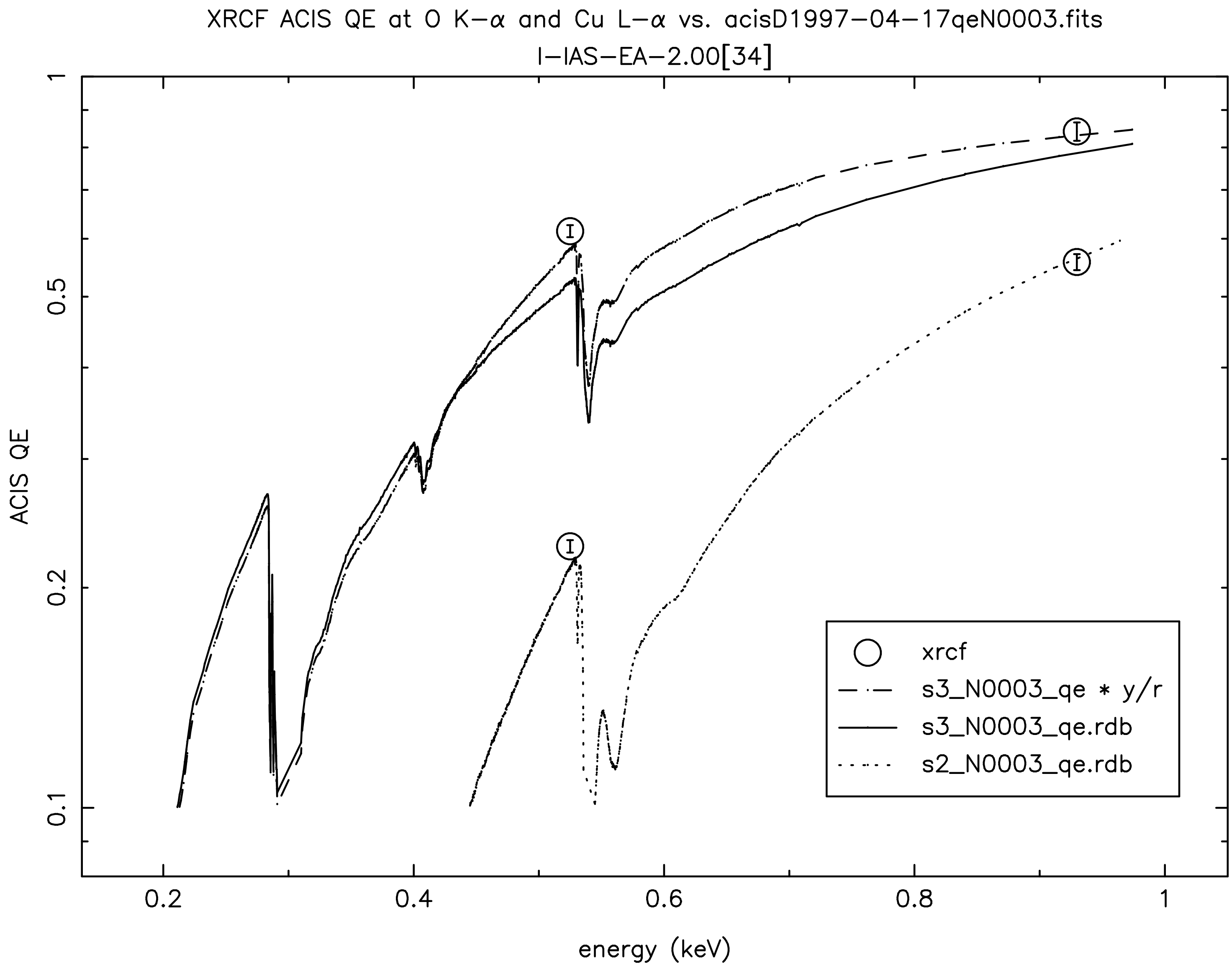

Figure 6: S2 and S3 quantum efficiency from CALDB N0003 (curves) and measured (data points). Now including corrected S3 QE curve for comparison.

Empirical QE Corrections

30 October 2001

- Compare Ball and Flight External Cal Source data
- Correct flight data for cosmic ray dead area effect
- Evidence for excess BI/FI ratio at Mn K–α
- Curvature of Marshall's suggested ratio correction around 700 eV not clear
- If S2 curve is right (as suggested at low energies), we propose the following empirical tweaks for the S3 QE:
  - **Low energies:** $QE'(E) = QE \times [1.05 - 0.16 \ln(E)]$
  - **High energies:** $QE'(E) = QE(E/1.05)$

ACIS QE BI/FI Ratio: Future Work

30 October 2001

- Correct FI QE curves by factor $y = 0.9632$ to account for cosmic ray blooms.
- Investigate CR bloom effect for BI chips, and correlations with other radiation measures.
- Analyze ground data at Fe L–α (0.705 keV), and at higher energies,notably Fe K–α (6.4 keV).
- Analyze ground data for BI chips at C K–α (to aid with extrapolation to low energy).
- Extend analysis to other chips (including the I array).

QEU Analysis Method

30 October 2001

- **Separate photons into two groups, FG=0,8,16,64,72,80,104,208 ("Good Good"), and FG=2,10,18,11,22 ("Bad Good")**
- **Good-Good photons migrate into good ASCA grades because of the CTI. The ECS intensity in the Good-Good grades is flat**
- **Bad-Good photons migrate into bad ASCA grades. QEU effects are stronger, easier to study.**
- **Derive energy dependence of the QEU for BAD-Good photons**

$$\log(QEU) \propto E \qquad \textbf{for BI chips}$$

$$QEU(E) \approx \mathrm{const} \qquad \textbf{for FI chips}$$

- **Derive spatial dependence of QE for the Mn-K complex: 1-column resolution for BI, 4-column resolution for FI.**
- **Derive energy dependence of the Bad-Good grade ratio in the total flux using ECS, E0102, G21.5, Perseus cluster, and ACIS simulator for FI chips.**
- **Final QEU maps:**

$$QEU(x,y,E) = QEU_{\mathrm{Mn}}(x,y)^{E/5.9} \times \mathrm{GradeRatio}(E) \qquad \textbf{for BI chips}$$

$$QEU(x,y,E) = QEU_{\mathrm{Mn}}(x,y) \times \mathrm{GradeRatio}(E) \qquad \textbf{for FI chips}$$

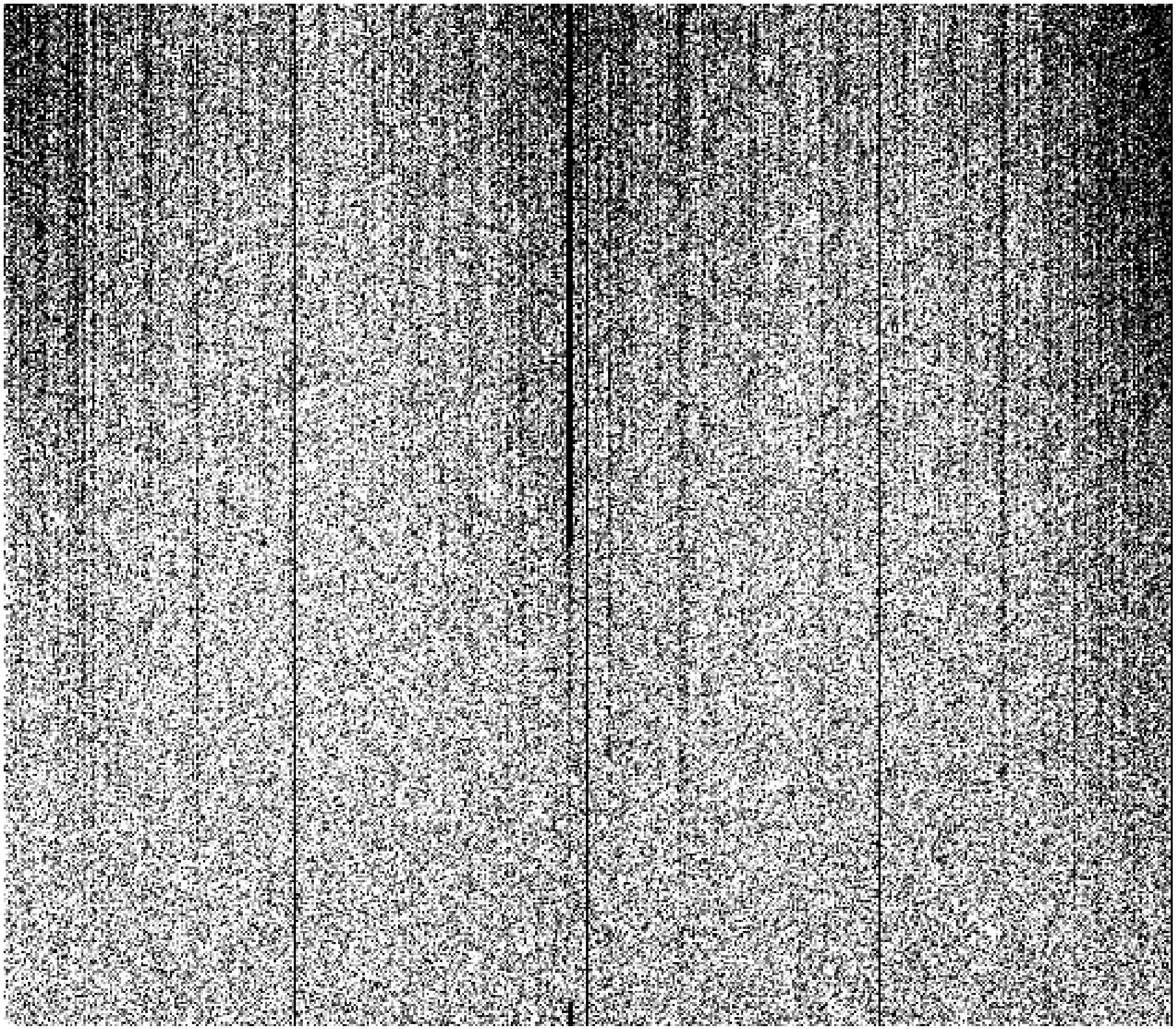

Figure 7: image of the S3 chip in the Mn K$\alpha + \beta$ lines, in the subset of ACIS grades that migrate into bad ASCA grades because of the CTI ("bad good" grades). Note strong column-to-column variations

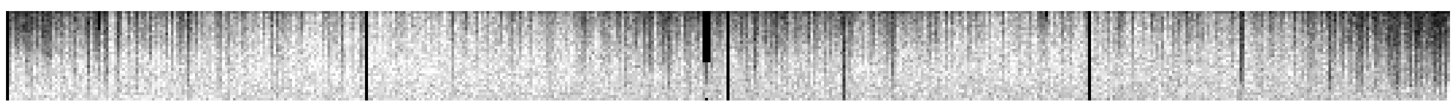

Figure 8: same as the previous one but binned by 16 along the chipy axis for clarity

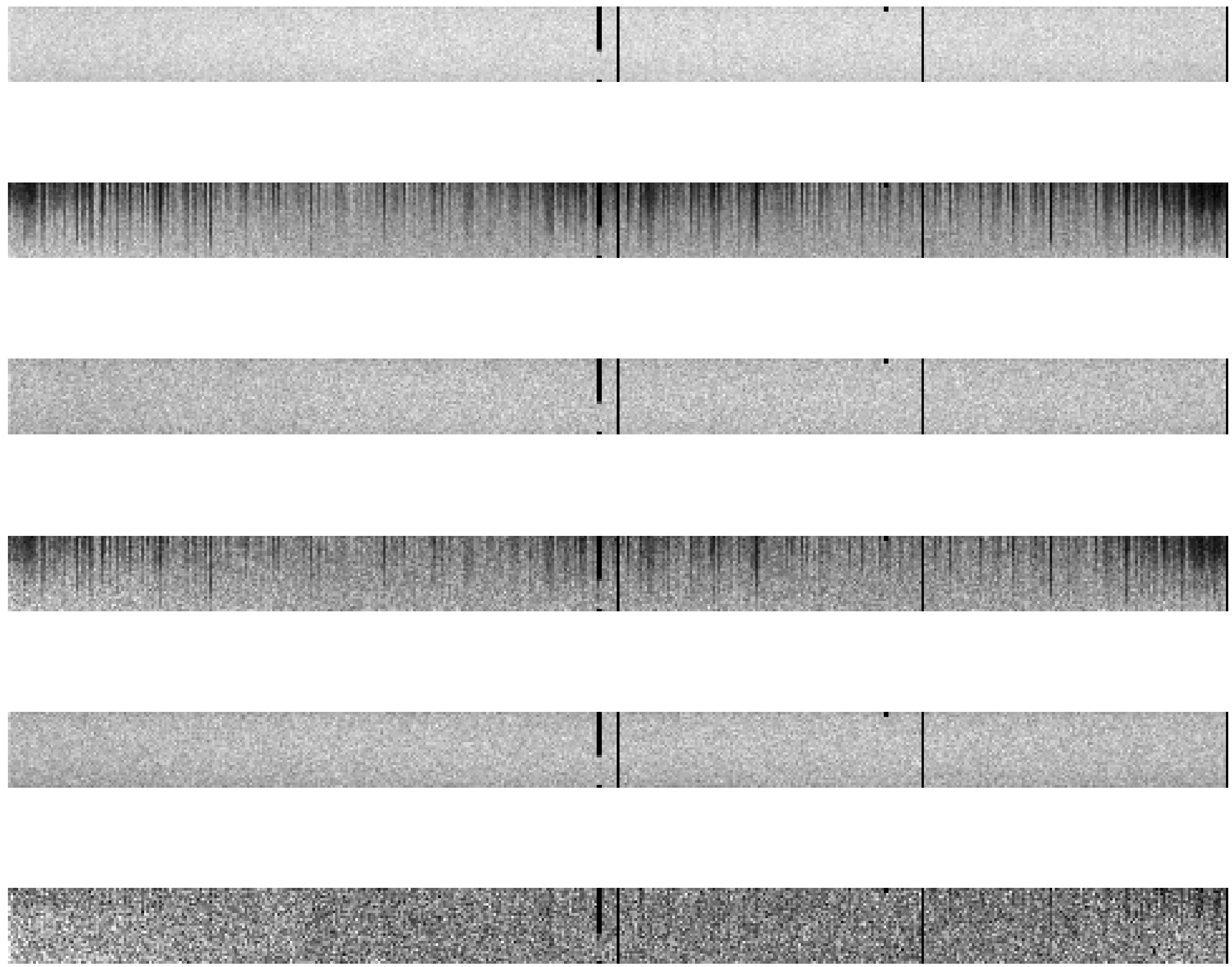

Figure 9: image of the S3 chips in the Mn, Ti, Al lines (top to bottom). The top image in each group is in the subset of grades which migrate into good ASCA grades ("good good" grades); the bottom one is for the "bad good" grades. Note flat images for "good good" grades and clear energy dependence of the QEU structure for the "bad good" grades.

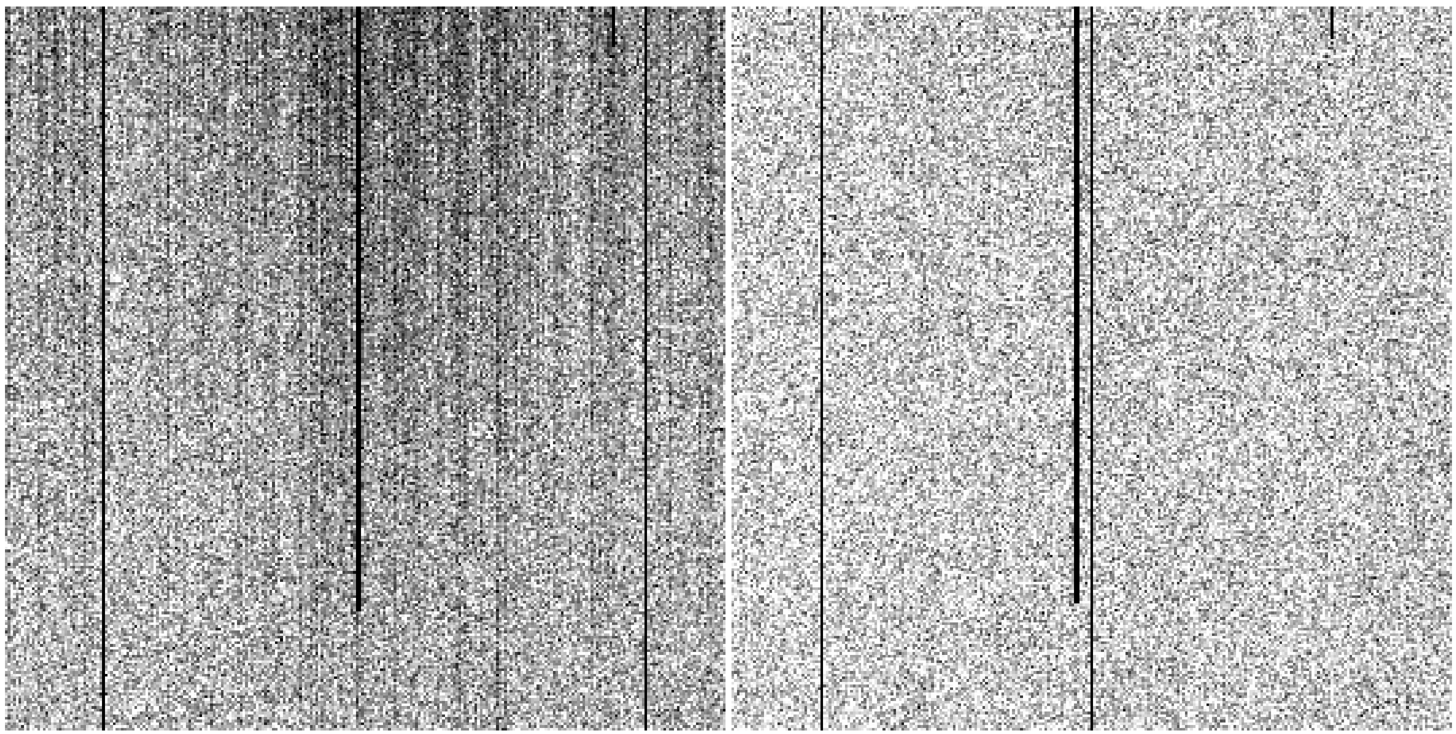

Figure 10: Image of the S3 chip in the MnK complex before and after the 1-column-resolution QEU correction.

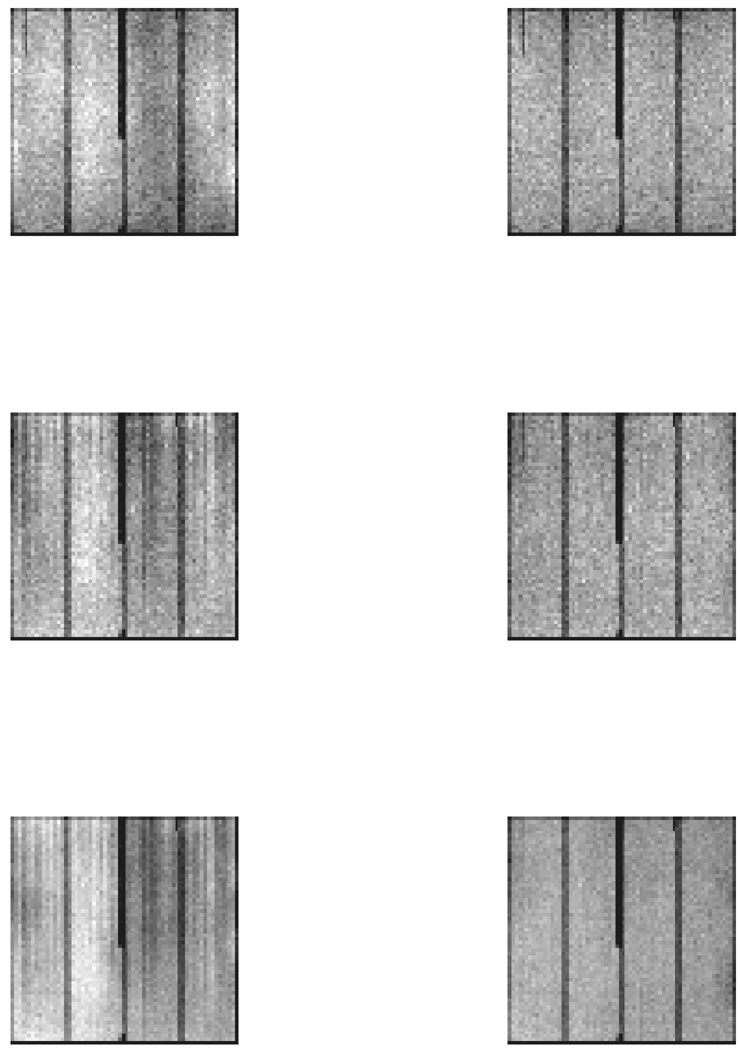

Figure 11: Results of the old and new QEU corrections to S3 in the Mn, Ti, and Al lines (top to bottom). Old is on the left and new is on the right

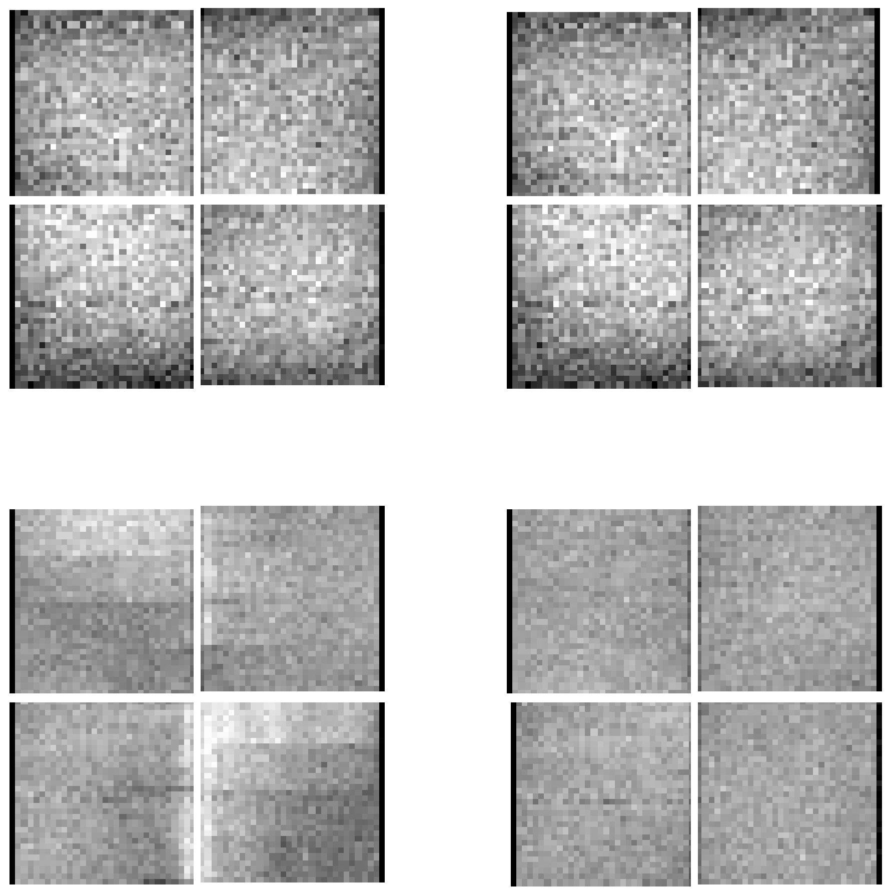

Figure 12: Same for the ACIS-I chips in Al (top) and Mn (bottom) lines.